Journal of Solid State Chemistry 184 (2011) 2215–2219

Contents lists available at ScienceDirect

Journal of Solid State Chemistry

journal homepage: www.elsevier.com/locate/jssc

Multifunctional properties of CoNi alloy embedded in the SiO_2 host: Role of interparticle interaction

S. Das, S. Majumdar, S. Giri *

Department of Solid State Physics, Indian Association for the Cultivation of Science, Jadavpur, Kolkata 700 032, India

ARTICLE INFO

Article history:
Received 10 February 2011
Received in revised form
21 June 2011
Accepted 26 June 2011
Available online 2 July 2011

Keywords:
Nanocrystalline materials
Alloy
Exchange bias
Magnetic hysteresis

ABSTRACT

Nanocrystalline CoNi alloy is synthesized using sol–gel technique having average size ~8.5 and ~12 nm. High-resolution transmission electron microscopy confirms absence of any oxide phase at the grain boundary. We observe multifunctionality ascribed to large loop shift after the field-cooling and saturation magnetization (M_S) depending on interparticle interaction in CoNi alloy embedded in SiO_2 matrix. A large loop shift 1.2 kOe is noticed at 5 K for 10.5% volume fraction (ϕ). The loop shift decreases with increasing temperature and vanishes around ~210 K where a maximum is observed in zero-field-cooled magnetization. The loop shift decreases with decreasing ϕ and vanishes at $\phi = 0.01\%$. Interestingly, M_S increases with decreasing ϕ and value at $\phi = 0.01\%$ approaches to the calculated value of M_S for the bulk counterpart. A model has been proposed with ferromagnetic-core and disordered magnetic-shell structure to interpret the results.

1. Introduction

Magnetic nanoparticles attract special attention for researchers from wide range of disciplines, including magnetic fluids [1], drug delivery [2], magnetic resonance imaging [3] and data storage [4]. In addition, fundamental issues on magnetism of nanoparticles are fascinating because of diverse range of magnetic properties depending on various factors such as size, shape, and anisotropy, interparticle interactions, and surface effects [5–7]. Collective states of interacting ferromagnetic (FM) nanoparticles [6] in association with non-equilibrium dynamics [7] have been discussed adequately where delicate interplay between interparticle interactions, particle size distributions, and effective anisotropy of individual particles leads to the diverse range of magnetic properties. Surface effect [8,9] is another key issue of nanoparticles which essentially results from lack of translational symmetry at boundaries of individual particle because of lower coordination number and existence of broken magnetic exchange bonds. These factors may lead to spin disorder or random spin canting associated with the occurrence of spin frustration. Moreover, anisotropic dipolar interaction in case of particles embedded in the nonmagnetic and insulating matrix favors ferromagnetic or antiferromagnetic alignments of the moments depending on geometry, which may give rise to necessary ingredients for the glassy magnetic states at the surface [5–7].

Recent observations of exchange bias (EB) effect in nanocrystalline oxides and alloys create a huge impact which can establish an evidence of strong surface effect [10]. Exchange bias effect is manifested by the loop shift after cooling sample in a static magnetic field attributed to the surface anisotropy, which has different magnetic anisotropy than the core magnetism, has been reported in various structurally single phase oxide nanocrystals such as NiO [11], CuO [12], iron oxides [13,14], cobalt oxides [15], spinels [17], cobalt ferrites [16] and mixed-valent manganites with perovskite structures [18,19]. This has been rarely reported in alloys [20–23]. In this article we report a large loop shift attributed to the surface effect in structurally single phase CoNi alloy having ~8.5 nm average size which are embedded in amorphous SiO_2 host. This loop shift being a typical manifestation of exchange bias effect is promising for the application [24,25]. Retaining size of the particle interparticle dipole–dipole (d–d) interaction has been tunned by controlling volume fraction (ϕ) of CoNi alloy in SiO_2 which resulted in significant change in loop shift, coercivity (H_C), and saturation magnetization (M_S). The dilution of particle leads to the significant decrease of loop shift and it disappears for $\phi = 0.01\%$. Strikingly, M_S increases systematically with decreasing ϕ. In fact, magnetization at 50 kOe is found to be ~1.27 μ_B/formula unit which is close to calculated value of M_S for the bulk counterpart (1.29 μ_B) [26]. The results demonstrate one of the finest way of improving magnetic properties of nanocrystalline compounds where strong EB effect manifested by loop shift ~1.2 kOe is found for dense particles and large M_S for low concentration of the particles. We propose magnetic core-shell structure to interpret the results where

* Corresponding author. Fax: +91 33 24732805.
E-mail address: sspsg2@iacs.res.in (S. Giri).

0022-4596/$ - see front matter © 2011 Elsevier Inc. All rights reserved.
doi:10.1016/j.jssc.2011.06.038

proportion of magnetic core and shell structure is strongly influenced by the volume fraction or interparticle d–d interaction.

2. Experimental details

Nanocrystalline CoNi alloy embedded in SiO_2 matrix was synthesized by standard sol–gel technique [27]. Stoichiometric ratios of cobalt nitrate and nickel nitrate are used for synthesis of CoNi alloy which were mixed with citric acid to achieve homogeneous metal citrate solution. Hydrolyzed ethanolic tetraethyl orthosilicate (TEOS) was used as source of SiO_2 which was added to the solution. The resulting clear solution was dried slowly to form a gel in air. The dried gel was decomposed at 550 and 800 °C for 5 h in a continuous flow of H_2/Ar gas mixture. The composition of the final product is $(Co_{0.99}Ni_{1.01})(SiO_2)_{10.4}$ with volume fraction, $\phi \approx 10.5\%$. This was confirmed using transmission electron microscopy (TEM) equipped with an energy dispersive X-ray (EDX) spectrometer (JEOL TEM, 2010) and atomic absorption spectroscopy (AAS) using a Shimadzu AA-6300 spectrometer. To record TEM image fine particles were dispersed in dehydrated alcohol and sonicated for a long period of time. One drop of cleared solution was spread over a carbon coated copper grid which was considered for recording TEM image. The TEM image of the particles decomposed at 550 °C is shown in Fig. 1. Average sizes of the particles are found to be ~8.5 and 12 nm when dried gel was decomposed at 550 and 800 °C, respectively. Herein, the experimental data for particles with average size at 12 nm is given only in the inset of Fig. 2(b). An example of high resolution TEM (HRTEM) image displaying planes until grain boundary region is shown in the upper inset of Fig. 1. HRTEM image confirms absence of any other structural phase ascribed to minor oxidation at the grain boundary region. The powder X-ray diffraction (XRD) studies were performed in a Seifert XRD 3000P diffractometer using Cu $K\alpha$ radiation source. The XRD pattern confirms the face-centered cubic structure ($Fm3m$) of CoNi alloy which is shown in the lower inset of figure. Magnetization measurements on pelletized sample were performed in a commercial SQUID magnetometer of Quantum Design (MPMS, XL). The value of magnetization is calculated from the actual composition obtained from AAS and EDX analyzes.

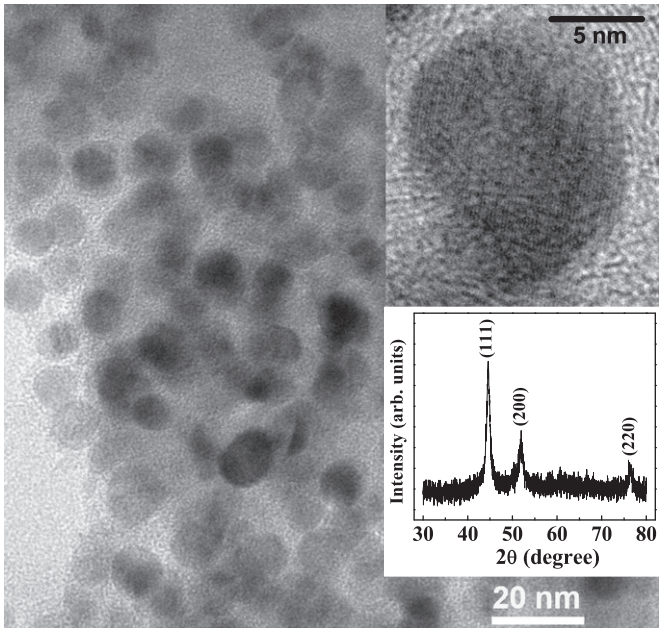

Fig. 1. TEM image of nanocrystalline CoNi alloy. Upper inset exhibits HRTEM image of a particle. Lower inset shows powder XRD pattern of CoNi alloy.

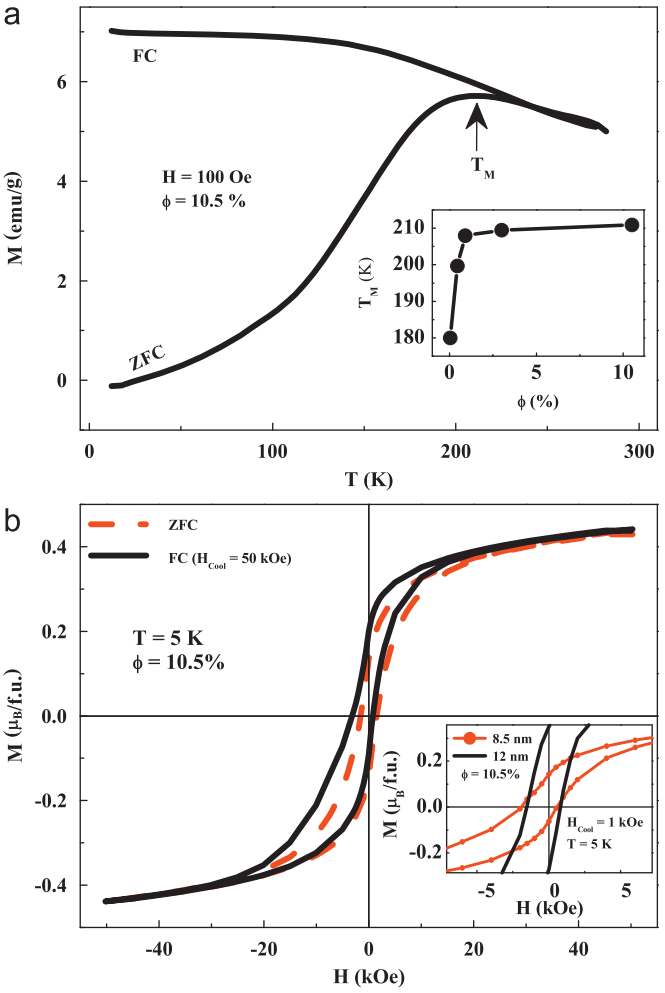

Fig. 2. (a) ZFC–FC effect of magnetization with temperature. Inset shows variation of T_M with volume fraction (ϕ). (b) Magnetic hysteresis loops at 5 K after cooling in ZFC and FC modes. Inset of (b) highlights the shifts of the hysteresis loops for nanocrystalline CoNi alloy at $\phi = 10.5\%$ with average size at 8.5 and 12 nm.

In case of measurement in zero-field-cooled (ZFC) mode sample was cooled in zero-field and measurement was carried out in the warming cycle in a static magnetic field. For field-cooled (FC) mode sample was cooled in field and measurement was carried out in the warming cycle like a ZFC measurement.

3. Experimental results and discussions

Temperature dependence of ZFC–FC magnetization measured at 100 Oe is shown in Fig. 2(a) for particles with $\phi = 10.5\%$. A broad maximum (T_M) appears at 210 K in the ZFC magnetization, above which ZFC and FC magnetization merge together. The results are in accordance with the previous report where a super-spin-glass like transition was proposed at T_M from the analysis of frequency dependent ac susceptibility results [28]. To investigate volume fraction dependent results ϕ were decreased systematically by adding SiO_2 to the sample with $\phi = 10.5\%$. To achieve nearly homogeneous mixture grinding was carried out in an agate mortar for long time period. In this process interparticle d–d interaction was tunned by controlling ϕ where physical size of the particles was remained same. We note that a rough estimate of the average interparticle distance is found to be ~10 nm for $\phi = 10.5\%$. As seen in the inset of Fig. 2(a) T_M decreases slowly and then it decreases sharply below $\phi = 0.9\%$.

Assuming that particles are physically separated by silica matrix, the exchange interactions among the particles may be neglected retaining the d–d interaction only. Practically, possibility of clustering or direct physical contact cannot be ruled out. However, such minor fraction does not influence dilution effect or decrease in volume fraction which is indicated by decrease of T_M in the inset of Fig. 2(a).

Moreover, we will notice in inset of Figs. 7 and 8 that physical parameters such as shifts of the magnetic hysteresis loops change systematically with ϕ. For a regular array of identical dipoles with identical magnetic moments μ the transition temperature is given by $T_M \approx (\mu_0 a_0/4\pi k_B)\mu M_S \phi$ [29,30], where M_S and μ are the saturation of magnetization and average moment of the magnetic nanoparticles, respectively, and a_0 strongly depends on particle size distribution. Here, T_M is the maximum observed in ZFC magnetization and considered that T_M appears due to dipole–dipole interaction only. Thus a_0 is close to 3.2. It was noted that $a_0 \approx 1$ for log-normal distribution function with distribution, $\sigma \approx 0.3$. The range of values of a_0 has been discussed to be in between 0.75 and 2.4 where particle size distribution was addressed for such wide range of values [29].

After cooling the sample ($\phi = 10.5\%$) in ZFC mode a symmetric magnetic hysteresis loop was recorded at 5 K which is shown in Fig. 2(b) by the broken curve. A considerable horizontal shift of the loop is observed at 5 K [continuous curve in Fig. 2(b)] when sample was cooled in FC mode. This is a typical manifestation of EB effect. The horizontal shift is ~ 1.2 kOe after field-cooling at $H_{cool}=50$ kOe. Shifts measured from the magnetic hysteresis loop may provide over-estimated value due to minor loop effect [31,32]. It has been pointed out that in case of minor loop anisotropy field, H_A is comparable to H_{max} where H_{max} is the maximum field used for the measurement of magnetic hysteresis loop. Herein, H_{max} has been considered at 50 kOe for each measurement which is $\gg H_A (\sim 18$ kOe) in the current investigation. Thus possibility of minor loop effect can be excluded in the current investigation. Inset of Fig. 2(b) exhibits example of loop shifts of nanocrystalline alloy with average size of 8.5 and 12 nm, retaining same volume fraction. We note that EB field is much smaller ~ 355 Oe for average size at 12 nm than that of the value ~ 667 Oe observed for 8.5 nm when samples were field-cooled at 1 kOe. This clearly demonstrates that larger surface effect likely for smaller particle provides larger loop shift. Training effect is commonly observed in a system exhibiting EB effect which is a consequence of decrease of loop shift with increasing number of field-cycling as demonstrated in Fig. 3(a). After cooling sample in $H_{cool}=3$ kOe down to 5 K magnetic hysteresis loop was measured seven times (i.e. index number, $\lambda = 7$) successively in between ± 50 kOe. Horizontal shift at zero magnetization defined as EB field (H_E) is plotted with $1/\sqrt{\lambda}$ in Fig. 3(b). The variation of H_E with λ could be fitted with the empirical formula, $H_E - H_E^{\infty} \propto 1/\sqrt{\lambda}$ for $\lambda \geq 2$ where H_E^{∞} is the value of H_E at $\lambda = \infty$. This is in accordance with the previous observations in various alloys and compounds [10,33–37]. Training effect can also be interpreted by the relaxation model proposed by Binek for all λ as $H_E(\lambda) - H_E(\lambda+1) = -\gamma[H_E(\lambda) - H_E(\lambda=\infty)]$ where γ is a constant [38]. Satisfactory fits of the simulated values of H_E (filled circles) with the experimental data (open circles) are shown in Fig. 3(b).

Plots of H_E and EB magnetization (M_E) defined as vertical shift at 50 kOe with temperature (T) are displayed in Fig. 4. H_E decreases with increasing T and vanishes around 210 K close to T_M for $\phi = 10.5\%$. Previous report suggests the super-spin-glass transition occurred at T_M [28]. Temperature dependence of loop shifts further demonstrates that EB effect is involved with the spin freezing below T_M. Above T_M spin frozen component cannot take part in the pinning mechanism. As a result of it EB vanishes at T_M. Horizontal shift was further recorded at 5 K after cooling in different H_{cool} which is shown in Fig. 5. The plot displays a sharp rise up to $H_{cool} \sim 30$ kOe and then it shows slow increasing trend

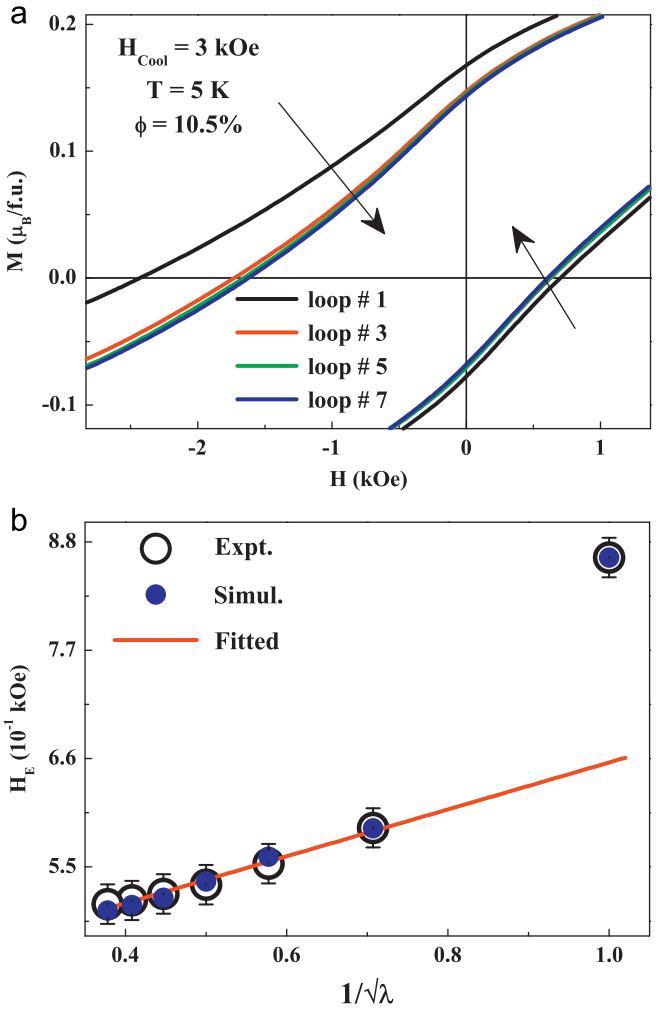

Fig. 3. (a) Training effect at 5 K where arrows indicate increasing direction of loop cycling. (b) Plots of H_E (open circles) with $1/\sqrt{\lambda}$. Filled circles show the simulated values using relaxation model. Straight line shows the fit using power law for $\lambda \geq 2$.

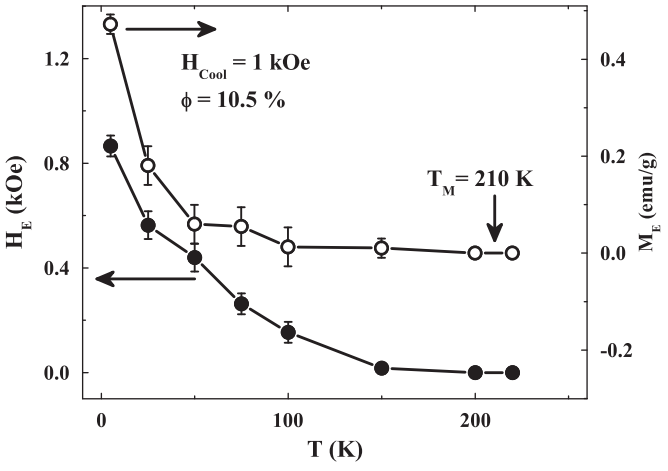

Fig. 4. Thermal (T) dependence of H_E and M_E of nanocrystalline CoNi alloy at $\phi = 10.5\%$.

up to $H_{cool}=50$ kOe. H_C follows an almost similar H_{cool} dependence as shown in Fig. 5. Thus increase of H_E is associated with the increase of overall anisotropy of the compound. Analogous to H_{cool} dependence of H_E, M_E follows a similar behavior. Niebieskikwiat and Salamon recently proposed a model based on simplified

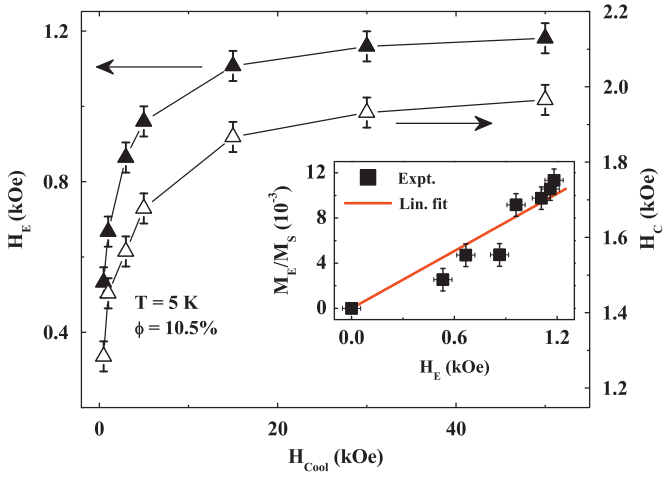

Fig. 5. Cooling field (H_{cool}) dependence of H_E and H_C for nanocrystalline CoNi alloy at $\phi = 10.5\%$. Inset shows the plot of M_E/M_S vs. H_E where straight line displays possible linear dependence.

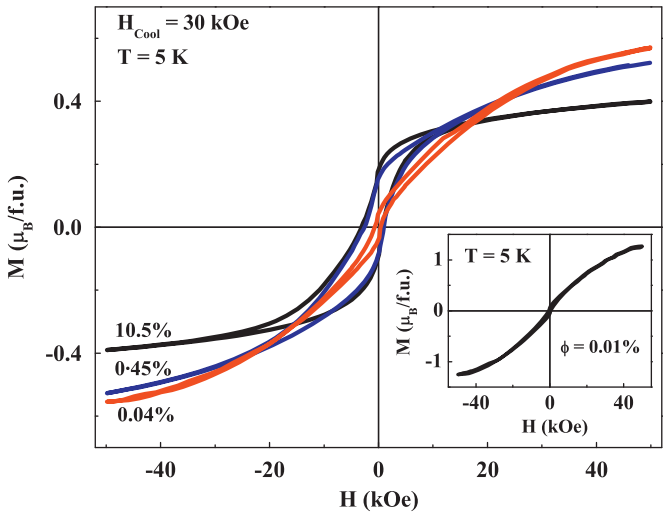

Fig. 6. Magnetic hysteresis loops at 5 K for $\phi = 0.04\%$, 0.45%, and 10.5% of nanocrystalline CoNi alloy. Inset shows the magnetic hysteresis loop for $\phi = 0.01\%$ at 5 K.

exchange interaction considering that noninteracting ferromagnetic nanoparticles having single magnetic domain are embedded in a non-ferromagnetic matrix [39]. The linear plot of H_E vs. M_E/M_S satisfying the model was demonstrated in $Pr_{1/3}Ca_{2/3}MnO_3$ [39] which has been also reported in different spontaneously phase separated systems [33–37]. The plot of H_E vs. M_E/M_S is shown in the inset of Fig. 5 which is not convincingly linear. Here, M_S is the saturation magnetization which is assumed to be close to the magnetization at 50 kOe.

We further investigated the study at different ϕ. Examples of magnetic hysteresis loops at 5 K for $\phi = 0.04\%$, 0.45%, and 10.5% are shown in Fig. 6. Interestingly, the values of magnetization at 50 kOe increase systematically with decreasing ϕ. In fact, magnetization at 50 kOe for $\phi = 0.01\%$ is $\sim 1.27\ \mu_B$/formula unit which approaches to the calculated value of M_S for the bulk counterpart (1.29 μ_B). This has been also observed for Co nanoparticles embedded in Ag and Mn matrixes where raise of M_S with decreasing ϕ was correlated with the combined d–d and RKKY interactions [40,41]. Here RKKY interaction does not occur, retaining only d–d interparticle interaction because insulating silica matrix exists physically in between the particles. We note

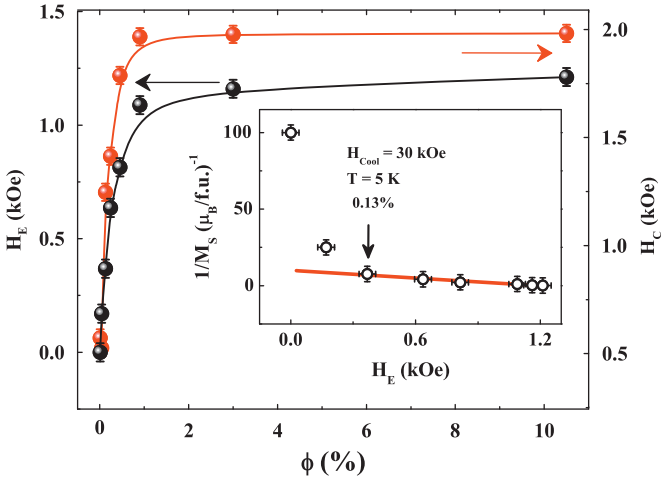

Fig. 7. The variation of H_E and H_C at 5 K with ϕ is displayed for nanocrystalline CoNi alloy. Inset shows the plot of $1/M_S$ against H_E at 5 K.

that H_C and H_E decrease with decreasing ϕ as shown in Fig. 7. To interpret the results we propose a magnetic core–shell structure where core is FM and shell is in disordered magnetic state as shown in the inset of Fig. 8. Exchange bias is suggested due to coupling between FM core and disordered magnetic shell in structurally single phase CoNi alloy. In fact, structurally single phase is confirmed by the HRTEM image. As seen in upper inset of Fig. 1 structural inhomogeneity is absent at the grain boundary region. The proposed magnetic core–shell model is consistent with the model proposed for FM core and disordered magnetic-shell structure to interpret loop shifts in nanoparticles of alloys [20–23]. Very recently, direct evidence of magnetic core–shell structure was reported in nanocrystalline magnetite from the small angle neutron studies [42]. This magnetic core–shell morphology was proposed due to d–d interaction between particles. Inset of Fig. 7 shows nearly linear plot of $1/M_S$ for different ϕ with the corresponding values of H_E i.e. H_E is inversely proportional to M_S for $\phi \geq 0.13\%$. This is consistent with the increase of magnetization at 50 kOe with decreasing ϕ where increase of FM size (decrease of disordered magnetic-shell thickness) leads to the enhancement of M_S. We note that EB effect vanishes at $\phi = 0.01\%$. The disordered magnetic-shell component almost disappears or weakens and thus EB effect is not observed. Assuming increase of M_S is proportional to the enhancement of volume fraction of FM core and FM core covers the whole physical size for $\phi = 0.01\%$, the values of D_{FM} are estimated with ϕ. Fig. 8 displays a linear plot of H_E with D_{FM}^{-1} except for the value at $\phi = 0.01\%$ which is consistent with the phenomenological relation, $H_E \propto 1/(D_{FM})^n$ with $n=1$. This relation was theoretically predicted [43] and experimentally verified with exponent, n in between 1 and 1.5 [25].

The influence of d–d interaction in the frozen ferrofluid has been investigated extensively where a crossover from superparamagnetic toward super-spin-glass behavior was associated with increasing d–d interaction as discussed from the dynamics of magnetization (frequency dependence of ac susceptibility and time dependence of magnetization) [44]. In fact, Monte Carlo simulations indicated that interparticle interactions are dominating enough to overcome the disorder induced by the distribution of anisotropy in dense nanoparticle assemblies [45]. We would like to emphasize that enhancement of collective glassy magnetic behavior was associated with the increase of d–d interaction. It has been realized that nature of this glassy magnetic behavior in the dense particle assemblies is not like conventional atomic spin-glass or cluster-glass [46]. Intrinsic magnetic structure of the dense system exhibiting collective glassy behavior is still elusive.

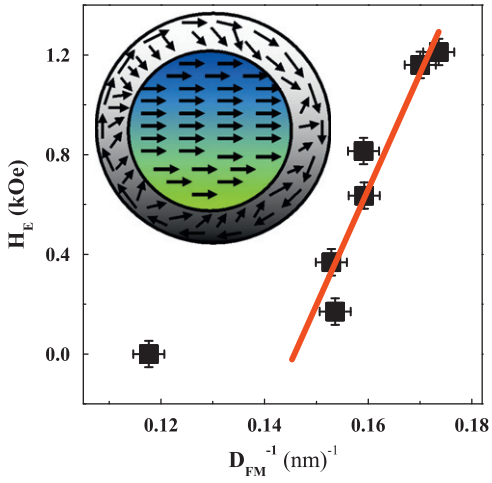

Fig. 8. Plot of H_E with D_{FM}^{-1} for nanocrystalline alloy. Inset exhibits the cartoon of FM-core and disordered magnetic-shell structure.

In this investigation, we propose a possible model from the systematic variation of H_E, H_C and M_S where stronger d–d interaction leads to the enhancement of glassy magnetic component and decrease of FM component of the nanoparticles. However, role of d–d interaction on the appearance of glassy magnetic state in terms of magnetic core–shell morphology needs to be verified from the theoretical and more experimental investigations using microscopic experimental tools.

4. Conclusion

In conclusion, we observe that tunning of interparticle interaction leads to the multifunctional properties in CoNi alloy embedded in SiO_2 matrix. A large loop shift is noticed for $\phi = 10.5\%$ which decreases with decreasing ϕ and vanishes at $\phi = 0.01\%$. At this most diluted volume fraction a large magnetization at 50 kOe and 5 K is observed which approaches to the bulk value of M_S. A FM-core and disordered magnetic-shell structure is proposed to interpret the observed loop shift at different ϕ. With decreasing ϕ FM size increases leading to the enhancement of M_S. The disordered magnetic phase at the surface almost disappears at $\phi = 0.01\%$ and exchange bias effect vanishes. Depending on the interparticle interaction large values of M_S and H_E in nanocrystalline CoNi alloy embedded in SiO_2 matrix are attractive for the technological applications.

Acknowledgment

One of the authors (S.G.) acknowledges Council of Scientific & Industrial Research (CSIR), India (Project No. 03(1167)/10/EMR-II) for the financial support. S.D. also wishes to thank CSIR, India for the Senior Research Fellowship.

References

[1] S. Chikazumi, S. Taketomi, M. Ukita, M. Mizukami, H. Miyajima, M. Setogawa, Y. Kurihara, J. Magn. Magn. Mater. 65 (1987) 245.
[2] J. Dobson, Gene Ther. 13 (2006) 283.
[3] Z. Li, L. Wei, M.Y. Gao, H. Lei, Adv. Mater. 17 (2005) 1001.
[4] G. Reiss, A. Hütten, Nat. Mater. 4 (2005) 725.
[5] J.L. Dormann, D. Fiorani, E. Tronc, Adv. Chem. Phys. XCVIII (1997) 283.
[6] O. Petracic, X. Chen, S. Bedanta, W. Kleemann, S. Sahoo, S. Cardoso, P.P. Freitas, J. Magn. Magn. Mater. 300 (2006) 192.
[7] P. Nordblad, J. Phys. D Appl. Phys. 41 (2008) 134011.
[8] Ó. Iglesias, A. Labarta, Physica B 343 (2004) 286.
[9] H. Kachkachi, E. Bonet, Phys. Rev. B 73 (2006) 224402.
[10] S. Giri, M. Patra, S. Majumdar, J. Phys. Condens. Mater. 23 (2011) 073201.
[11] S.K. Sharma, J.M. Vargas, E.D. Biasi, F. Béron, M. Knobel, K.R. Pirota, C.T. Meneses, S. Kumar, C.G. Lee, P.G. Pagliuso, C. Rettori, Nanotechnology 21 (2010) 035602.
[12] A. Punnoose, H. Magnone, M.S. Seehra, J. Bonevich, Phys. Rev. B 64 (2001) 174420.
[13] T.N. Shendruk, R.D. Desautels, B.W. Southern, J. van Lierop, Nanotechnology 18 (2007) 455704.
[14] G. Salazar-Alvarez, J. Qin, V. Šepelák, I. Bergmann, M. Vasilakaki, K.N. Trohidou, J.D. Ardisson, W.A.A. Macedo, M. Mikhaylova, M. Muhammed, M.D. Baró, J. Nogués, J. Am. Chem. Soc. 130 (2008) 13234.
[15] M.J. Benitez, O. Petracic, E.L. Salabas, F. Radu, H. Tüysüz, F. Schüth, H. Zabel, Phys. Rev. Lett. 101 (2008) 097206.
[16] D. Peddis, C. Cannas, G. Piccaluga, E. Agostinelli, D. Fiorani, Nanotechnology 21 (2010) 125705.
[17] H.T. Zhang, X.H. Chen, Nanotechnology 17 (2006) 1384.
[18] V. Markovich, I. Fita, A. Wisniewski, D. Mogilyansky, R. Puzniak, L. Titelman, C. Martin, G. Gorodetsky, Phys. Rev. B 81 (2010) 094428.
[19] T. Zhang, M. Dressel, Phys. Rev. B 80 (2009) 014435.
[20] A. Hernando, E. Navarro, M. Multigner, A.R. Yavari, D. Fiorani, M. Rosenberg, G. Filoti, R. Caciuffo, Phys. Rev. B 58 (1999) 5181.
[21] D.L. Leslie-Pelecky, R.L. Schalek, Phys. Rev. B 59 (1999) 457.
[22] I. Škorvánek, R. Grössinger, J. Magn. Magn. Mater. 226–230 (2001) 1473.
[23] C.H. Ho, C.H. Lai, IEEE Trans. Magn. 42 (2006) 3069.
[24] J. Nogués, I.K. Schuller, J. Magn. Magn. Mater. 192 (1999) 203.
[25] J. Nogues, J. Sort, V. Langlais, V. Skumryev, S. Surinach, J.S. Munoz, M.D. Baro, Phys. Rep. 422 (2005) 65.
[26] C. Kittel, Introduction to Solid State Physics, John Wiley & Sons, Inc., New York, 1976.
[27] G. Mattei, C. de Julián Fernández, P. Mazzoldi, C. Sada, G. De, G. Battaglin, C. Sangregorio, D. Gatteschi, Chem. Mater. 14 (2002) 3440.
[28] M. Thakur, M. Patra, S. Majumdar, S. Giri, J. Appl. Phys. 105 (2009) 073905.
[29] M.F. Hansen, S. Morup, J. Magn. Magn. Mater. 184 (1998) 262.
[30] S. Morup, Europhys. Lett. 28 (1994) 671.
[31] J. Geshev, J. Magn. Magn. Mater. 320 (2008) 600.
[32] M. Patra, M. Thakur, K. De, S. Majumdar, S. Giri, J. Phys. Condens. Mater. 21 (2009) 078002.
[33] M. Patra, S. Majumdar, S. Giri, Europhys. Lett. 87 (2009) 58002.
[34] M. Patra, M. Thakur, S. Majumdar, S. Giri, J. Phys. Condens. Mater. 21 (2009) 236004.
[35] M. Patra, S. Majumdar, S. Giri, Solid State Commun. 149 (2009) 501.
[36] M. Patra, S. Majumdar, S. Giri, J. Phys. Condens. Mater. 21 (2009) 486003.
[37] M. Patra, S. Majumdar, S. Giri, J. Appl. Phys. 107 (2010) 033912.
[38] Ch. Binek, Phys. Rev. B 7 (2004) 014421.
[39] D. Niebieskikwiat, M.B. Salamon, Phys. Rev. B 72 (2005) 174422.
[40] N. Domingo, A.M. Testa, D. Fiorani, C. Binns, S. Baker, J. Tejada, J. Magn. Magn. Mater. 316 (2007) 155.
[41] N. Domingo, D. Fiorani, A.M. Testa, C. Binns, S. Baker, J. Tejada, J. Phys. D Appl. Phys. 41 (2008) 134009.
[42] K.L. Krycka, R.A. Booth, C.R. Hogg, Y. Ijiri, J.A. Borchers, W.C. Chen, S.M. Watson, M. Laver, T.R. Gentile, Phys. Rev. Lett. 104 (2010) 207203.
[43] M.D. Stiles, R.D. McMichael, Phys. Rev. B 63 (2001) 064405.
[44] C. Djurberg, P. Svedlindh, P. Nordblad, M.F. Hansen, F. Bodker, S. Morup, Phys. Rev. Lett. 79 (1997) 5154.
[45] Ó. Iglesias, A. Labarta, Phys. Rev. B 70 (2004) 144401.
[46] J.A. Mydosh, Spin Glasses: An Experimental Introduction, Taylor and Francis, London, 1993.